ROYAL SOCIETY
OF CHEMISTRY

PAPER

Check for updates

A novel metal–organic framework of Ba–hemin with enhanced cascade activity for sensitive glucose detection†

Jintao Yi, [ID] *[a] Xianqin Han,[a] Fengying Gao,[a] Le Cai,[a] Ying Chen,[a] Xiulong Deng,[a] Xun Li,*[a] Jun Xue*[a] and Hui Zhou [ID] *[ab]

Early glucose detection is important in both healthy people and diabetic patients. Glucose biosensing based on glucose oxidase (GOX) is a common method. However, native proteins are mostly membrane impermeable and are prone to degradation in complex sample environments. Herein, we report a facile one-step biomineralization method by simply mixing aqueous solutions of hemin and barium nitrate with glucose oxidase (GOX) to form Ba–hemin@GOX composites. Glucose (Glu) is introduced through self-driven sampling to trigger the GOX-catalysed production of hydrogen peroxide, which could help the subsequent 3,3′,5,5′-tetramethylbenzidine (TMB) oxidation reaction catalysed by Ba–hemin to yield the blue-coloured product. The sensor exhibited a detection limit as low as 3.08 μM. The operability and accuracy of the Ba–hemin@GOX biosensor were confirmed by the quantitative determination of glucose in real samples, such as tap water, serum and drinks. Moreover, the Ba–hemin@GOX-based colorimetric biosensor showed good selectivity, storage stability and recoverability. The experimental results reveal that a GOX activity of more than 90% was still maintained even after being incubated at 60 °C for 30 minutes, and Ba–hemin@GOX could be reused for glucose detection at least six times. Even after 30 days of storage, the relative activity was still more than 90%. Overall, the developed Ba–hemin@GOX biosensor provides a valuable and general platform for applications in colorimetric biosensing and medical diagnostics.

1 Introduction

Glucose plays an important role in metabolism and serves as an energy source for the body and brain. An abnormal blood glucose level in the body may lead to serious diseases, the most common of which is diabetes.[1] As a chronic disease, diabetes can lead to serious complications, which endanger the life of patients.[2] Therefore, the accurate and timely detection of glucose levels in diabetes patients is of great significance. The glucose detection methods based on conventional analytical instruments such as high-performance liquid chromatography (HPLC), gas chromatography (GC) and capillary zone electrophoresis (CZE) have the advantages of accuracy and reliability but have shortcomings such as complex operation and expensive instruments.[3] Electrochemical methods for glucose detection based on the electrodes of metals and metal nanomaterials

exhibit good sensitivity and low limits of detection but have poor selectivity and instability of electrodes by the interference of other species.[4] Enzymatic methods for glucose detection, particularly GOX-based sensors, have been widely studied and extensively applied in practice, with the merits of high sensitivity, excellent selectivity and low cost.[5] However, these enzymatic methods face the challenge of the activity and stability of native enzymes being easily affected by external environmental factors (such as temperature, pH and humidity). Thus, a reliable means to maintain enzyme activity is expected to improve the performance of enzymatic sensors.

Proteins have evolved to self-assemble into quaternary structures due to their supramolecular nature, which can protect the genome from environmental challenges including extreme temperature, extreme pH, radiation and digesting enzymes.[6] Proteins can be self-assembled by supramolecular strategies. Supramolecular coordination complexes, which are formed *via* the weak-link approach (WLA),[7,8] have found wide applications in catalysis, small molecule recognition and transportation.[9–12] Such systems can encapsulate the protein, create a nanoscale environment to increase the speed of a chemical reaction, affect oligomerization processes and alter reaction routes. In these systems, a small molecule reacts at the

[a]Key Laboratory of Organo-Pharmaceutical Chemistry of Jiangxi Province, Gannan Normal University, Ganzhou 341000, P. R. China. E-mail: yistarthappy@163.com; Fax: +86-797-8393536; Tel: +86-797-8393536

[b]Guangdong Provincial Key Laboratory of Research and Development of Natural Drugs, School of Pharmacy, Guangdong Medical University, Dongguan 523808, P. R. China

† Electronic supplementary information (ESI) available. See https://doi.org/10.1039/d2ra02778j

allosteric regulatory site to regulate the activity of catalysts by changing the supramolecular structure.

Metal–organic frameworks (MOFs), a class of highly crystalline inorganic–organic hybrids constructed by self-assembled organic ligands and metal ions, have attracted immense attention owing to their finely tunable chemical composition, pore size and shape, and accessible specific surface areas.[13–15] Supramolecular coordination complexes based on MOFs have emerged as valuable materials and have been widely applied in gas storage, catalysis, separation, encapsulation and the delivery of chemical drugs.[16–20] These studies have encouraged us to construct a glucose biosensor using MOFs as the immobilizing matrix to load GOX. Since hemin is a catalytic porphyrin with two carboxylate groups that can form coordinative bonds with metal ions, it is hypothesised that this organic ligand may aid the synthesis of MOFs with peroxidase-like properties.[21] As we know, glucose is catalysed by glucose oxidase (GOX) and generates the product H_2O_2.[22] These studies inspire us to construct a hemin-MOF with GOX with tandem catalysis for glucose detection. A colorimetric sensor has the merits of simple operation, fast response and visible colour changes, which are good for observing target signals by the naked eye.[23]

Herein, a novel Ba–hemin MOF with excellent catalytic activity towards the catalytic decomposition of H_2O_2 was fabricated *via* Ba^{2+} coordination with hemin. Then, a novel one-step biomineralization method was fabricated by simply mixing aqueous solutions of hemin and barium nitrate along with glucose oxidase (GOX) to form Ba–hemin@GOX metal-organic-framework composites for colorimetric glucose biosensing. GOX molecules were incorporated into the Ba–hemin MOFs, which effectively avoided the degradation of the native enzyme that was exposed to the environment. The Ba–hemin@GOX composites could not only catalyse the oxidization of glucose *via* GOX and generate the product H_2O_2 but also catalyse the decomposition of H_2O_2 *via* the Ba–hemin MOFs effectively, which could promote the colour change of 3,3′,5,5′-tetramethylbenzidine (TMB) from colourless to blue. This unique colorimetric biosensor based on the tandem catalysis of GOX and the Ba–hemin mimic enzyme has been utilized successfully to detect glucose in actual samples.

2 Experimental section

2.1 Materials and reagents

Barium nitrate ($Ba(NO_3)_2$) and hemin were purchased from Sigma-Aldrich. Glucose oxidase (GOX), xylose, pectinose, fructose, agarose, glucose, galactose, sucrose, rhamnose, mannose, dialysis membranes (MWCO 20k) and 3,3′,5,5′-tetramethylbenzidine (TMB) were bought from Sangon Biological Engineering Technology & Services Company Ltd. (Shanghai, China). All other reagents were of analytical grade. Ultrapure water was obtained through a Millipore Milli-Q water purification system (Billerica) with an electrical resistance > 18.25 MΩ.

2.2 Apparatus

The UV spectra were recorded on a UV-2700 UV-visible spectrophotometer (Shimadzu Instrument Inc., Japan). The crystal phase of the nanoparticles was identified by scanning electron microscopy (Bruker, Germany). The Fourier transform infrared (FTIR) spectra were recorded with a spectrometer. The crystal phase of the nanoparticles was determined using a D8-Advance X-ray diffractometer (Bruker, Germany). A TG 209 F1 Libra thermogravimetric analyzer (Netzsch, Germany) was used for thermogravimetric analysis (TGA). The fluorescence spectra were recorded using a FluoroMax-4 spectrofluorometer (HORIBA Jobin Yvon, Inc., NJ).

2.3 Synthesis of Ba–hemin

According to a previous report, Ba–hemin was synthesized with some modification.[24] Typically, 1.31 g barium nitrate was dissolved in 15 mL H_2O, and 3.26 mg hemin was dissolved in another 15 mL H_2O. After appropriate ultrasonication, the two solutions were mixed under vigorous stirring at 37 °C for 2 h. The resulting solution was centrifuged at 7000 rpm for 30 min, washed twice with water and dried at 60 °C to obtain bulk Ba–hemin particles.

2.4 Synthesis of Ba–hemin@GOX

Typically, 600 mg glucose oxidase (GOX) was first added in an aqueous solution of hemin (3.26 mg, 15 mL) under vigorous stirring and incubated at 37 °C for 10 min. Then, an aqueous solution of barium nitrate (1.31 g, 15 mL) was mixed with the above mixture and stirred at 37 °C for 2 h. The obtained Ba–hemin@GOX particles were washed with a 5% SDS (w/w) aqueous solution to remove free proteins from the surface and redispersed in 30 mL 3% PVP (w/w) aqueous solutions. The concentration of the obtained Ba–hemin@GOX particles was about 0.32 mg mL^{-1}. Finally, the as-prepared PVP-coated Ba–hemin@GOX particles were stored at 4 °C for future use.

2.5 The determination of the loading amount of GOX in Ba–hemin

GOX was marked with fluorescein isothiocyanate (FTIC). The FITC-labelled GOX was prepared by mixing 10 mg mL^{-1} GOX in 0.1 M phosphate buffer (PB, pH 8.0) with 1 mg mL^{-1} FITC at 37 °C for 2 h; then, the mixed solution was purified using dialysis membranes to obtain the enriched FITC-labelled GOX. Ba–hemin@FITC-GOX was synthesized following the procedure mentioned above. To determine the protein encapsulation efficiency, the fresh SDS-washed Ba–hemin@FITC-GOX particles were firstly suspended in 1 mL 1× HEPES buffer (25 mM HEPES, 137 mM NaCl, pH 5.5) for 2 h to release the encapsulated protein *via* acidic decomposition. The resulting solution was treated with an ultrafiltration device (Millipore, 10k) at 7000 rpm for 30 min and washed twice using ultrapure water. Then, the fluorescence intensity of the supernatant solution was measured. The encapsulation efficiency of the proteins was calculated using the ratios of the fluorescence intensity of the proteins collected from the Ba–hemin@FITC-GOX particles to

the fluorescence intensity of the FITC-GOX provided in the synthesis.

2.6 The detection of glucose by free GOX and Ba–hemin@GOX

The activity of Ba–hemin@GOX and free GOX was determined. In a typical assay, 10 μL 3,3′,5,5′-tetramethylbenzidine (TMB) solution (10 mM), 20 μL glucose (5.55 mM), 37 μL HAc–NaAc buffer (0.4 M, pH 4.5), and 20 μL Ba–hemin@GOX (0.32 mg mL^{-1}) or GOX (0.04 mg mL^{-1}) were added sequentially into 63 μL sterile water, and the mixture was incubated at 25 °C for 10 min. Then, the changes in the absorbance at 652 nm were recorded over time.

In the assay of glucose detection, 10 μL 3,3′,5,5′-tetramethylbenzidine (TMB) solution (10 mM), 37 μL HAc–NaAc buffer (0.4 M, pH 4.5), and 20 μL Ba–hemin@GOX (0.32 mg mL^{-1}) were added sequentially into 63 μL sterile water. Subsequently, a series of different concentrations of glucose (20 μL) were added to the above mixture and incubated for 10 min at 25 °C. Next, the absorbance was recorded at 652 nm.

Then, the kinetic parameters were determined. Firstly, 20 μL glucose solution with different concentrations (0.018 mM, 0.037 mM, 0.074 mM, 0.185 mM, 0.37 mM and 0.555 mM) were mixed with 20 μL Ba–hemin@GOX (0.32 mg mL^{-1}), 10 μL 3,3′,5,5′-tetramethylbenzidine (TMB) solution (10 mM), 37 μL HAc–NaAc buffer (0.4 M, pH 4.5) and 63 μL sterile water. The absorbance of the mixture solution at 652 nm was recorded immediately and the changes in the absorbance at 652 nm over time were recorded.

2.7 Effect of immobilization on the GOX activity in Ba–hemin@GOX

Firstly, 20 μL Ba–hemin@GOX (0.32 mg mL^{-1}) was treated with different temperatures (37 °C, 60 °C, 100 °C) for 30 min. Then, 10 μL 3,3′,5,5′-tetramethylbenzidine (TMB) solution (10 mM), 37 μL HAc–NaAc buffer (0.4 M, pH 4.5), 20 μL glucose (5.55 mM) and 63 μL sterile water were added to the pretreated solution of Ba–hemin@GOX. Finally, the mixture was incubated at 25 °C for 10 min, and the absorbance was measured at 652 nm.

To determine the effects of pH, 20 μL Ba–hemin@GOX (0.32 mg mL^{-1}) was treated with different pH conditions (4–10) for 30 min. Then, the pretreated solution of Ba–hemin@GOX was mixed with 10 μL 3,3′,5,5′-tetramethylbenzidine (TMB) solution (10 mM), 37 μL HAc–NaAc buffer (0.4 M, pH 4.5) and 20 μL glucose (5.55 mM). The absorbance was recorded at 652 nm after incubating at 25 °C for 10 min.

2.8 The selectivity, recoverability and storage stability of Ba–hemin@GOX

The selectivity of Ba–hemin@GOX was evaluated by monitoring the changes in the absorbance at 652 nm in the presence of different sugars. The sugars included xylose, pectinose, fructose, agarose, galactose, sucrose, rhamnose, and mannose. The recoverability of Ba–hemin@GOX was evaluated by cyclic glucose detection. When the first detection was completed, after washing and centrifugation, Ba–hemin@GOX was reused in the next determination process. The storage stability of Ba–hemin@GOX was evaluated by separately storing it in PBS and sterile water. After 1 day, 15 days and 30 days, the activity of the stored Ba–hemin@GOX was tested by recording the absorbance at 652 nm.

2.9 Practical detection in tap water, serum and drink

Before use, three real samples of tap water, serum and drink were diluted ten times. In a typical assay, 63 μL of the above diluted sample, 10 μL 3,3′,5,5′-tetramethylbenzidine (TMB) solution (10 mM), 37 μL HAc–NaAc buffer (0.4 M, pH 4.5), 20 μL glucose (5.55 mM) and 20 μL Ba–hemin@GOX (0.32 mg mL^{-1}) were incubated at 25 °C for 10 min, and the absorbance was measured at 652 nm. Each sample was measured three times.

3 Results and discussion

3.1 Design and characterization

In this work, as shown in Scheme 1, the Ba–hemin@GOX composites were firstly synthesized by mixing glucose oxidase, barium nitrate and hemin. Then, glucose (Glu) was introduced through self-driven sampling to trigger the GOX-catalysed production of H$_2$O$_2$, which was subsequently degraded via a catalytic reaction with the peroxidase-like activity of Ba–hemin. This catalytic reaction produces the hydroxyl radical, which can help the subsequent 3,3′,5,5′-tetramethylbenzidine (TMB) oxidation reaction to yield a blue-coloured product.

The morphology of Ba–hemin was revealed by scanning electron microscopy (SEM). As shown in Fig. S1,† the synthesis of Ba–hemin was optimized in terms of the molar ratio between Ba^{2+} ions and hemin. As this ratio increased from 50 to 2000, the MOF of Ba–hemin gradually became monodispersed and reached maximum productivity at a ratio of 1000. Under the optimal conditions, the synthesized Ba–hemin exhibited a flower-like morphology and had an average length of about 5 μm. Fig. S2† shows the UV-vis absorbance spectra of hemin and Ba–hemin MOF. The absorption peak of hemin appeared at 385 nm. However, the absorption peak of Ba–hemin showed a redshift with a wider absorption range between 400 and
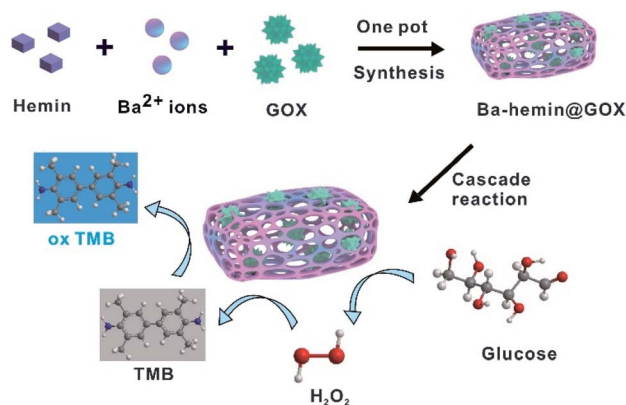
Scheme 1 Illustration of the Ba–hemin@GOX composite for glucose detection.

700 nm, probably due to the stronger conjugate interaction inside Ba–hemin MOF. The kinetic parameters, Michaelis–Menten constant (K_m) and maximum reaction rate (V_{max}) of Ba–hemin were determined by the Lineweaver–Burk plot of $1/V$–$1/C$. As shown in Fig. S3A,† under the same concentration of H_2O_2, the absorbance values of TMB at 652 nm increased continuously, and at the same response time, the reaction rates increased with increasing concentration of H_2O_2. The K_m value and V_{max} of Ba–hemin were 19 mM and 0.5 μM s^{-1}, respectively (Fig. S3B†). For comparison, the K_m value and V_{max} of free horseradish peroxidase (HRP) were 2.4 mM and 2.3 μM s^{-1}, respectively (Fig. S4†). The kinetic parameters of Ba–hemin and HRP were quite close, indicating that Ba–hemin had good peroxidase-like catalytic activity.

With this excellent catalytic activity, Ba–hemin was developed for the cascade catalytic reaction. As we know, glucose oxidase (GOX) can catalyse the production of H_2O_2; thus, GOX was used as an example.[22] The morphology of Ba–hemin@GOX was detected by scanning electron microscopy (SEM). The results show that Ba–hemin@GOX possesses similar flower-like structures, but Ba–hemin@GOX has a larger diameter of about 10 μm (Fig. 1A) due to the facilitated aggregative growth kinetics mediated by GOX-seeded clusters, which allowed the formation of large crystals. The chemical structures of Ba–hemin and Ba–hemin@GOX were detected by Fourier-transform infrared (FTIR) spectroscopy. As shown in Fig. 1B, the characteristic absorption band of hemin was observed at 1690 cm^{-1} (purple vertical line), ascribed to the –COOH group. Unlike in hemin, the –COOH bonds (1690 cm^{-1}) of Ba–hemin and Ba–hemin@GOX all disappeared due to the coordination of the carboxyl groups between hemin and the barium ions. The crystalline structures of Ba–hemin and Ba–hemin@GOX were revealed by X-ray diffraction (XRD) (Fig. 1C). The XRD data confirm that Ba–hemin@GOX retained the same crystalline form as that of pure Ba–hemin, suggesting that the crystalline structure of Ba–

hemin was not altered by a minor amount of proteins. The thermal stability of Ba–hemin and Ba–hemin@GOX were determined by thermogravimetric analysis (TGA). The results show that Ba–hemin remained stable at about 250 °C (Fig. S5,† black curve), and the thermal stability of Ba–hemin@GOX was slightly worse than that of Ba–hemin (Fig. S5,† red curve) owing to a change in the structure of the enzyme during the heating process. Taken together, these results demonstrate that using a one-pot synthetic method, the biomimetic mineralization method provided facile, fast and consistent synthesis of Ba–hemin@GOX composites.

To ascertain that the biomimetic mineralization synthesis indeed produced GOX-encapsulated particles, the as-prepared Ba–hemin@GOX particles were washed with sodium dodecylsulfate (SDS), which is known to remove surface-bound proteins from particles, followed by Fourier transform infrared spectroscopy (FTIR) (Fig. S6†). For Ba–hemin@GOX (GOX proteins wrapped in Ba–hemin) and Ba–hemin/GOX (GOX proteins adsorbed at the surface of Ba–hemin), the absorption bands characteristic of GOX were still observed in the range of $\sim$1640 to 1660 cm^{-1} (brown vertical line), ascribed to the amide I band. In contrast, the FTIR spectrum from the control sample prepared by mixing pre-formed pure Ba–hemin crystals and GOX followed by washing with SDS did not give the characteristic band, and a similar result was obtained for Ba–hemin. Taken together, these results demonstrate that the biomimetic mineralization synthesis indeed produced GOX-encapsulated particles.

3.2 Effect of immobilization on GOX activity in Ba–hemin@GOX

The protein encapsulation efficiency was investigated by fluorescence detection. The GOX protein was tagged using FITC (fluorescein isothiocyanate isomer, a fluorescence dye). When FITC-GOX was wrapped in Ba–hemin, the fluorescence intensity of Ba–hemin@GOX (the FITC-GOX protein in Ba–hemin, red curve) and the unreacted FITC-GOX (black curve) were detected (Fig. S7†). The relative amount of protein encapsulated in Ba–hemin@FITC-GOX to the amount of protein initially provided for the synthesis of Ba–hemin@FITC-GOX was calculated to be $\sim$59.17%.

Furthermore, the kinetic parameters, Michaelis–Menten constant (K_m) and maximum reaction rate (V_{max}) of Ba–hemin@GOX were determined by the Lineweaver–Burk plot of $1/V$–$1/C$. As shown in Fig. S8,† the K_m values of free GOX and Ba–hemin@GOX were 2.12 mM and 2.23 mM, respectively. The K_m value of Ba–hemin@GOX was higher than that of free GOX, indicating that the affinity of the enzyme to the substrate had decreased after immobilization. The V_{max} values of free GOX and Ba–hemin@GOX were 2.92 × 10^{-8} M s^{-1} and 2.77 × 10^{-8} M s^{-1}, respectively. The V_{max} value decreased in Ba–hemin@GOX compared with that of free GOX, implying the reduced catalytic activity and lower substrate accessibility to the active site after immobilization. These results were comparable to previously reported results.[25]

Moreover, the effect of temperature and pH on the activity of Ba–hemin@GOX was also explored. As shown in Fig. S9,† the
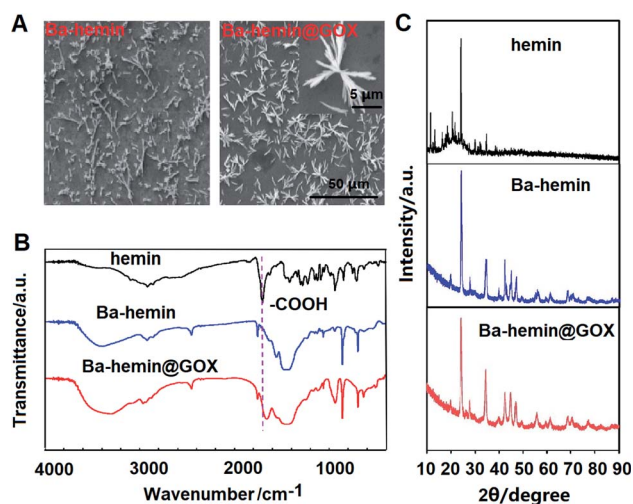

Fig. 1 Characterization of particles. (A) SEM images of Ba–hemin and Ba–hemin@GOX. (B) FTIR spectra of hemin, Ba–hemin and Ba–hemin@GOX. (C) XRD patterns of hemin, Ba–hemin and Ba–hemin@GOX.

results showed that Ba–hemin@GOX exhibited higher activity than free GOX from 30 °C to 60 °C, indicating that the temperature tolerance of GOX was improved after immobilization in Ba–hemin. In addition, compared to free GOX, the acid–base tolerance of Ba–hemin@GOX was also enhanced in the pH range of 4–10. In short, the immobilization of GOX on Ba–hemin could reduce the influence of environmental challenges on enzyme activity and enhance the tolerance of GOX in extreme conditions.

3.3 The performance of the Ba–hemin@GOX biosensor

The peroxidase-like activity of Ba–hemin was investigated by the oxidation reaction of 3,3′,5,5′-tetramethylbenzidine (TMB). As shown in Fig. 2, with H_2O_2, the TMB solution exhibited high absorbance at 652 nm (dark yellow curve), indicating that Ba–hemin could catalyse the decomposition of H_2O_2. As we know, glucose can be catalysed by GOX to produce H_2O_2. When we added glucose, GOX and Ba–hemin together, the colour of the TMB solution changed from colourless to blue (yellow curve), indicating the synergistic catalytic function of GOX and Ba–hemin. To improve the stability of GOX, a facile one-step biomineralization method by simply mixing aqueous solutions of hemin and barium nitrate with glucose oxidase (GOX) to form Ba–hemin@GOX composites was proposed. The feasibility of Ba–hemin@GOX for the detection of glucose was investigated. As shown in Fig. 2, in the presence of glucose, a high absorbance signal at 652 nm was shown (cyan curve). By contrast, without glucose, a weak absorbance signal was generated (purple curve), and similar weak signals of other control samples were obtained, indicating both the GOX and peroxidase-like activities of Ba–hemin@GOX.

Under the optimized experimental conditions, the performance of Ba–hemin@GOX for glucose was investigated. With the increase in the target glucose concentration from 0 to 1.5 mM, the absorbance of TMB increased gradually (Fig. 3A), with a linear range from 9.25 μM to 0.74 mM (Fig. 3B). The detection limit was estimated to be 3.083 μM (in terms of the rule of 3 times deviation over the blank response). Compared with reported glucose colorimetric sensors, this method displayed a wider linear range and relatively lower detection limit, as listed in Table S1.†[26–30]
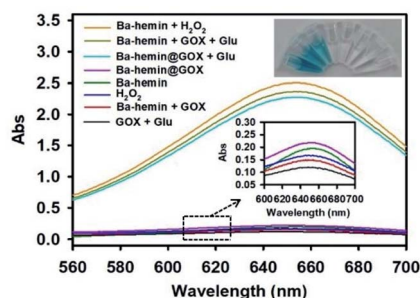

Fig. 2 The UV spectra of TMB solutions at 650 nm in response to different samples.
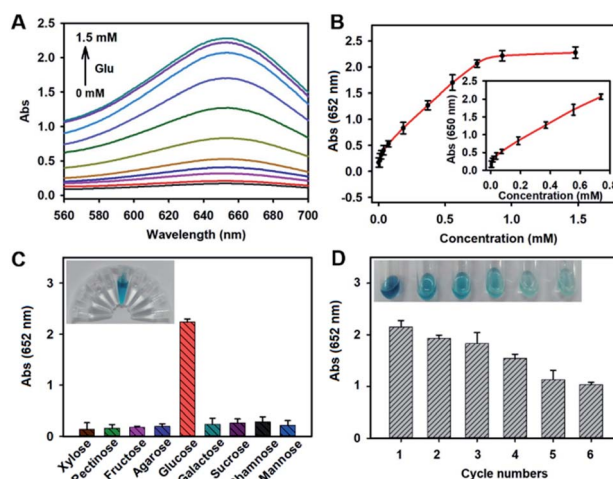

Fig. 3 The glucose detection by Ba–hemin@GOX. (A) The UV spectra of TMB solutions at 652 nm in response to different concentrations of glucose. (B) The relationship between the UV absorbance and the amount of glucose. Inset: linear relationship between the UV absorbance and the amount of glucose. Error bars represent the standard deviation of three parallel experiments. (C) The selectivity of Ba–hemin@GOX to xylose (5 mM), pectinose (5 mM), fructose (5 mM), agarose (5 mM), galactose (5 mM), sucrose (5 mM), rhamnose (5 mM), mannose (5 mM) and glucose (2 mM). (D) The recyclability of Ba–hemin@GOX.

The selectivity of Ba–hemin@GOX to glucose was investigated by testing the changes in the absorbance at 652 nm with glucose analogues, namely xylose, pectinose, fructose, agarose, galactose, sucrose, rhamnose and mannose. As can been seen from Fig. 3C, even though the concentrations of the glucose analogues were 2.5 times higher than that of glucose, the absorbance values of the glucose analogue samples at 652 nm were still lower than that of the glucose sample. These results could be clearly seen by the naked eye, indicating the good selectivity of Ba–hemin@GOX, due to Ba–hemin-enwrapped GOX, which was specific for glucose detection, and Ba–hemin@GOX could create a nanoscale environment to increase the reaction rate of the cascade catalytic reaction.

Next, the reusability of Ba–hemin@GOX was investigated by recycling and reuse experiments. Ba–hemin@GOX was recycled by simply washing and centrifuging, and then used for the next detection cycle. The results in Fig. 3D show that Ba–hemin@GOX still retained an activity of more than 70% after four detection cycles. Furthermore, the storage stability of Ba–hemin@GOX was investigated in PBS and water. After being kept in PBS for 30 days, the relative activity of Ba–hemin@GOX was still more than 90% (Fig. S10†), implying the good stability of Ba–hemin@GOX.

To further investigate the accuracy and practicability of Ba–hemin@GOX-based colorimetric biosensors, the concentrations of glucose in tap water, serum and drink samples were detected. Each sample was tested three times. As shown in Table S2,† the glucose concentrations in tap water, serum and drink samples obtained with the Ba–hemin@GOX-based biosensor were quite consistent with the added glucose concentrations; the recovery rate was in the range of 92–110.8%,

and the experimental standard deviations were in the range of 1.5–5.4%. These results prove that the Ba–hemin@GOX colorimetric biosensor is suitable for glucose detection in real samples.

4 Conclusions

In summary, we developed biomineralized Ba–hemin particles encapsulating GOX as a novel platform with cascade activity for sensitive glucose detection. By finely controlling the concentration ratio of hemin to Ba^{2+}, a novel one-pot synthetic method was applied by encapsulating nanoscale proteins in Ba–hemin. This encapsulation structure has the advantages of preserving protein activity, improving storage stability and displaying good reusability. Moreover, the Ba–hemin@GOX-based biosensor exhibited a wide linear range of 9.25 μM to 0.74 mM and a relatively low detection limit of 3.083 μM. Moreover, the Ba–hemin@GOX-based colorimetric biosensor was successfully applied in actual samples, such as tap water, serum and drink. This work expands the range of enzyme-functionalized MOF materials and demonstrates that Ba–hemin@GOX is promising for use in colorimetric biosensing and medical diagnostics.

Author contributions

Jintao Yi: methodology, writing-original draft, funding acquisition. Xianqin Han and Fengying Gao: project administration, data curation. Le Cai and Ying Chen: software, formal analysis. Xiulong Deng: methodology. Xun Li, Jun Xue and Hui Zhou: writing-review & editing, funding acquisition. All authors have read and agreed to the published version of the manuscript.

Conflicts of interest

The authors declare no competing financial interest.

Acknowledgements

References

1 J. Xu, K. K. Xu, Y. Han, D. Wang, X. Li, T. Hu, H. Yi and Z. H. Ni, *Analyst*, 2020, **145**(15), 5141–5147.

2 X. Wei, J. Chen, M. C. Ali, J. C. Munyemana and H. D. Qiu, *Mikrochim. Acta*, 2020, **187**(6), 314–318.

3 M. Y. Ma, Y. Zhou, J. H. Li, Z. Q. Ge, H. P. He, T. Tao, Z. W. Cai, X. B. Wang, G. Chang and Y. B. He, *Analyst*, 2020, **145**(3), 887–896.

4 L. Q. Kong, D. Wang, Y. Q. Chai, Y. L. Yuan and R. Yuan, *Anal. Chem.*, 2019, **91**(15), 10289–10294.

5 S. Yoo, K. Min, G. Tae and M. S. Han, *Nanoscale*, 2021, **13**(8), 4467–4474.

6 Y. S. Bai, Q. Luo and J. Q. Liu, *Chem. Soc. Rev.*, 2016, **45**(10), 2756–2767.

7 H. J. Yoon, J. Heo and C. A. Mirkin, *J. Am. Chem. Soc.*, 2007, **129**(46), 14182–14183.

8 H. J. Yoon and C. A. Mirkin, *J. Am. Chem. Soc.*, 2008, **130**(35), 11590–11591.

9 H. J. Yoon, J. Kuwabara, J. H. Kim and C. A. Mirkin, *Science*, 2010, **330**(6000), 66–69.

10 J. Chen, S. Körner, S. L. Craig, S. Lin, D. M. Rudkevich and J. R. Jr, *Proc. Natl. Acad. Sci. U. S. A.*, 2002, **99**(5), 2593–2596.

11 N. C. Gianneschi, S. B. T. Nguyen and C. A. Mirkin, *J. Am. Chem. Soc.*, 2005, **127**(6), 1644–1645.

12 C. M. Soto, A. S. Blum, G. J. Vora, N. Lebedev, C. E. Meador, A. P. Won, A. Chatterji, J. E. Johnson and B. R. Ratna, *J. Am. Chem. Soc.*, 2006, **128**(15), 5184–5189.

13 H. Furukawa, K. E. Cordova, M. O'Keeffe and O. M. Yaghi, *Science*, 2013, **341**(6149), 1230444–1230448.

14 Q. H. Yang, Q. Xu, S. H. Yu and H. L. Jiang, *Angew. Chem., Int. Ed. Engl.*, 2016, **55**(11), 3685–3689.

15 N. Stock and S. Biswas, *Chem. Rev.*, 2012, **112**(2), 933–969.

16 T. T. Chen, J. T. Yi, Y. Y. Zhao and X. Chu, *J. Am. Chem. Soc.*, 2018, **140**(31), 9912–9920.

17 Y. Q. Yin, C. L. Gao, Q. Xiao, G. Lin, Z. Lin, Z. W. Cai and H. H. Yang, *ACS Appl. Mater. Interfaces*, 2016, **8**(42), 29052–29061.

18 M. Adeel, K. Asif, M. M. Rahman, S. Daniele, V. Canzonieri and F. Rizzolio, *Adv. Funct. Mater.*, 2021, **31**(1), 2106023–2106051.

19 C. Hou, Y. Wang, Q. H. Ding, L. Jiang, M. Li, W. W. Zhu, D. Pan, H. Zhu and M. Z. Liu, *Nanoscale*, 2015, **7**(44), 18770–18779.

20 Y. Yue, X. L. Ding, L. Wang, R. Yang, J. S. Bi, Y. W. Song, P. Yang, Y. Ma and B. Tang, *Mater. Chem. Front.*, 2021, **5**(1), 3859–3866.

21 N. Alizadeh, A. Salimi, R. Hallaj, F. Fathi and F. Soleimani, *J. Nanobiotechnol.*, 2018, **16**(1), 93–97.

22 T. Tzanov, S. A. Costa, G. M. Gubitz and A. C. Paulo, *J. Biotechnol.*, 2002, **93**(1), 87–94.

23 S. He, Q. T. Huang, Y. Zhang, H. F. Zhang, H. F. Xu, X. Li and X. M. Ma, *Chin. Chem. Lett.*, 2021, **32**(4), 1462–1465.

24 L. Mi, Y. D. Sun, L. Shi and T. Li, *ACS Appl. Mater. Interfaces*, 2020, **12**(7), 7879–7887.

25 A. K. Haskell, A. M. Sulman, E. P. Golikova, B. D. Stein, M. Pink, D. G. Morgan, N. V. Lakina, A. Y. Karpenkov, O. P. Tkachenko, E. M. Sulman, V. G. Matveeva and L. M. Bronstein, *ACS Omega*, 2020, **5**(21), 12329–12338.

26 H. Wei and E. K. Wang, *Anal. Chem.*, 2008, **80**(6), 2250–2254.

27 X. G. Luo, J. Xia, X. Y. Jiang, M. R. Yang and S. L. Liu, *Anal. Chem.*, 2019, **91**(24), 15461–15468.

28 J. Xu, K. K. Xu, Y. Han, D. Wang, X. Li, T. Hu, H. Yi and Z. H. Ni, *Analyst*, 2020, **145**(15), 5141–5147.

29 J. Soto, T. Hughes and Y. S. Li, *ACS Omega*, 2019, **4**(19), 18312–18316.

30 H. Q. Zheng, C. Y. Liu, X. Y. Zeng, J. Chen, J. Lü, R. G. Lin, R. Cao, Z. J. Lin and J. W. Su, *Inorg. Chem.*, 2018, **57**(15), 9096–9104.